Eur. Phys. J. A **20**, 257–262 (2004)
DOI 10.1140/epja/i2003-10151-x

THE EUROPEAN PHYSICAL JOURNAL A

Different effect of the hyperons Λ and Ξ on the nuclear core

Yu-Hong Tan[1,a] and Ping-Zhi Ning[2]

[1] Theoretical Physics Division, Nankai Institute of Mathematics, Nankai University, Tianjin 300071, PRC
[2] Department of Physics, Nankai University, Tianjin 300071, PRC

Received: 10 March 2003 / Revised version: 6 November 2003 /
Published online: 5 May 2004 –
Communicated by A. Molinari

Abstract. We demonstrate the different effect of strange impurities (Λ and Ξ) on the static properties of nuclei within the framework of the relativistic mean-field model. Systematic calculations show that the glue-like role of the Λ-hyperon is universal for all Λ-hypernuclei considered. However, the Ξ^--hyperon has a glue-like role only for the protons distribution in nuclei, while for the neutrons distribution it plays a repulsive role. On the other hand, the Ξ^0-hyperon attracts the surrounding neutrons and reveals a repulsive force to the protons. Possible explanations of the above observation are discussed.

PACS. 21.80.+a Hypernuclei – 24.10.Cn Many-body theory

1 Introduction

The change of the bulk properties of nuclei under the presence of strange impurities, like the lambda-hyperon (Λ), is an interesting subject in hypernuclear physics. Since Λ does not suffer from Pauli blocking, it can locate at the center of a nucleus, then it attracts the surrounding nucleons (the glue-like role of Λ) and makes the nucleus shrink. One might expect only a small change of size for most of the nuclei. However, significant shrinkage of the hypernuclei size could be expected when a Λ is added to loosely bound light nuclei such as ^{6}Li [1–3]. Recently, the experiment KEK-PS E419 has found clear evidence for this shrinkage of the hypernucleus $^7_\Lambda$Li [4,5].

In order to obtain a more profound understanding of the glue-like role of strange impurities in nuclei, it is necessary to consider other strange impurities, like Σ and Ξ. The behavior of these hyperons in the nuclear medium, as well as the hyperon-nucleus potential, is of particular importance for this study. However, the Σ-nucleus potential continues to be unclear until recent times because the experimental information is limited [6]. For the sake of improving this situation, a new experiment at KEK has been carried out to measure the inclusive (π^-, K^-) spectrum, which is sensitive to the Σ-nucleus potential [7]. The result shows that a strongly repulsive Σ-nucleus potential is required to reproduce the observed spectrum. So, we have reason to believe that the Σ-hyperon does not have any glue-like role and cannot make the nucleus shrink. Next in mass are the Ξ^-- and Ξ^0-hyperons. Experimental evidence suggests that the Ξ-nucleus potential is attractive [8]. Therefore we may only consider Λ- and Ξ-hypernuclei in this work. Our purposes are i) to test the universality of the glue-like role of the Λ impurity in a variety of Λ-hypernuclei which may not be loosely bound light nuclei; ii) to see whether or not the Λ and Ξ impurities behave the same, in view of the fact that both Λ and Ξ nuclear potentials are attractive; iii) to predict the properties of the Ξ impurities in Ξ-hypernuclei.

To accomplish this, a standard approach to the subject is the relativistic mean-field (RMF) model, a brief description of which for the hypernuclei is given in sect. 2. In sect. 3, after testing the validity of force parameters used in the RMF model, systematic calculations are performed for Λ-hypernuclei and the universality of the glue-like role of the Λ impurity is revealed. In sect. 4, we provide the RMF results for the Ξ-hypernuclei and different effects of Ξ^- and Ξ^0 on the nucleus are discussed. A brief summary is made and conclusions are drawn in sect. 5.

2 The RMF model

The relativistic mean-field model (RMF) has been used to describe nuclear matter, finite nuclei, and hypernuclei successfully. Here, we start from a Lagrangian density of the form

$$\mathcal{L} = \mathcal{L}_N + \mathcal{L}_\mathrm{y}, \tag{1}$$

[a] e-mail: htan@nankai.edu.cn

where y = Λ, Ξ^-, Ξ^0 and $\mathcal{L}_N$ is the standard Lagrangian of the RMF model:

$$\begin{aligned}\mathcal{L}_N = \bar{\psi}_N\Big(&i\gamma_\mu\partial^\mu - M_N - g_{\sigma N}\sigma - g_{\omega N}\gamma_\mu\omega^\mu \\ &-\frac{1}{2}g_{\rho N}\gamma_\mu\vec{\tau}_N\cdot\vec{\rho}^{\,\mu} - e\gamma_\mu\frac{1+\tau_{3,N}}{2}A^\mu\Big)\psi_N \\ &+\frac{1}{2}(\partial_\mu\sigma\partial^\mu\sigma - m_\sigma^2\sigma^2) \\ &-\frac{1}{3}b\sigma^3 - \frac{1}{4}c\sigma^4 \\ &-\frac{1}{4}\Omega_{\mu\nu}\Omega^{\mu\nu} + \frac{1}{2}m_\omega^2\omega_\mu\omega^\mu \\ &-\frac{1}{4}\vec{R}_{\mu\nu}\cdot\vec{R}^{\mu\nu} + \frac{1}{2}m_\rho^2\vec{\rho}_\mu\cdot\vec{\rho}^{\,\mu} \\ &-\frac{1}{4}H_{\mu\nu}\cdot H^{\mu\nu}\,, \end{aligned} \tag{2}$$

where

$$\begin{aligned}\Omega_{\mu\nu} &= \partial_\nu\omega_\mu - \partial_\mu\omega_\nu\,, \\ \vec{R}_{\mu\nu} &= \partial_\nu\vec{\rho}_\mu - \partial_\mu\vec{\rho}_\nu\,, \\ H_{\mu\nu} &= \partial_\nu A_\mu - \partial_\mu A_\nu\,. \end{aligned} \tag{3}$$

It involves nucleons (ψ_N), scalar σ-mesons (σ), vector ω-mesons (ω_μ), vector-isovector ρ-mesons ($\vec{\rho}_\mu$), and the photon (A_μ). The scalar self-interaction $-\frac{1}{3}b\sigma^3 - \frac{1}{4}c\sigma^4$ is included as well. The parametrization of the nucleonic sector (NL-SH) is adopted from ref. [9], the properties of finite nuclei can be well described.

The Lagrangian density $\mathcal{L}_\Lambda$ describes the hyperon ψ_Λ and its coupling to mesonic fields includes the ω-Λ tensor coupling term:

$$\begin{aligned}\mathcal{L}_\Lambda = &\bar{\psi}_\Lambda(i\gamma^\mu\partial_\mu - m_\Lambda - g_{\sigma\Lambda}\sigma - g_{\omega\Lambda}\gamma_\mu\omega^\mu)\psi_\Lambda \\ &+\frac{f_{\omega\Lambda}}{2m_{\rm y}}\bar{\psi}_\Lambda\sigma_{\mu\nu}\cdot\partial^\nu\omega^\mu\psi_\Lambda. \end{aligned} \tag{4}$$

Since Λ is a neutral and isoscalar baryon, it does not couple with the ρ-mesons and the photon. We adopt the parametrization of the Λ sector from ref. [10]: $g_{\sigma\Lambda}/g_{\sigma N} = 0.49, g_{\omega\Lambda}/g_{\omega N} = 0.512, f_{\omega\Lambda}/g_{\omega\Lambda} = -0.616$. Using these coupling constants, the properties of the Λ-hypernuclei can be well described [10,11].

The Lagrangian density $\mathcal{L}_\Xi$ describes the hyperon ψ_Ξ and its couplings to the σ, ω , ρ mesonic fields and the photon field:

$$\begin{aligned}\mathcal{L}_\Xi = \bar{\psi}_\Xi\Big(&i\gamma^\mu\partial_\mu - m_\Xi - g_{\sigma\Xi}\sigma - g_{\omega\Xi}\gamma_\mu\omega^\mu \\ &-\frac{1}{2}g_{\rho\Xi}\gamma_\mu\vec{\tau}_\Xi\cdot\vec{\rho}^{\,\mu} - e\gamma_\mu\frac{\tau_{3,\Xi}-1}{2}A^\mu\Big)\psi_\Xi\,. \end{aligned} \tag{5}$$

We fix the coupling constants of Ξ, say the one to the vector fields with the quark model ($SU(6)$ symmetry),

$$g_{\omega\Xi} = \frac{1}{3}g_{\omega N}, \tag{6}$$

$$g_{\rho\Xi} = g_{\rho N}, \tag{7}$$

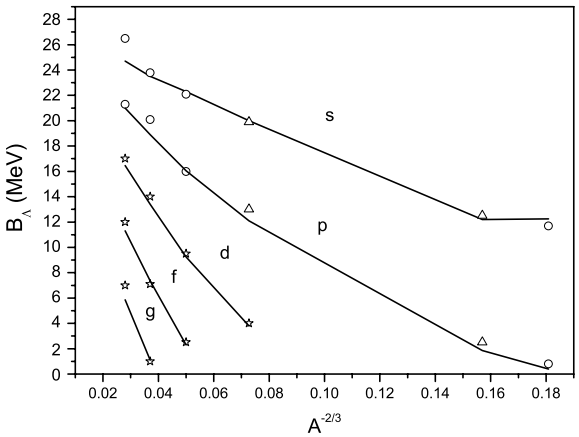

Fig. 1. Λ binding energies (in MeV) for some hypernuclei ($^{13}_{\Lambda}$C, $^{16}_{\Lambda}$O, $^{51}_{\Lambda}$V, $^{89}_{\Lambda}$Y, $^{139}_{\Lambda}$La, $^{208}_{\Lambda}$Pb). The solid lines are our RMF results with the parameters of ref. [10]. The experimental data are taken from ref. [16], ref. [17], and ref. [18] denoted by △, ○, ☆, respectively.

and those to the scalar field with the experimental information —the optical potential. It turns out that two coupling constants of Ξ, $g_{\sigma\Xi}$ and $g_{\omega\Xi}$ are strongly correlated because they are fixed by the depth of the Ξ potential:

$$V_0^\Xi = g_{\sigma\Xi}\sigma^{eq} + g_{\omega\Xi}\omega^{eq} \tag{8}$$

in the saturation nuclear matter [12,13]. But the experimental data on the Ξ^--hypernuclei are very few. Dover and Gal [14], analyzing old emulsion data on the Ξ^--hypernuclei, arrive at a nuclear potential well depth $V_0^\Xi = -21\cdots-24$ MeV. Fukuda *et al.* [15] fit to the very low-energy part of the Ξ^- hypernuclear spectrum in the ^{12}C(K$^-$, K$^+$)X reaction in experiments E224 at KEK and estimate the value of V_0^Ξ to be between -16 and -20 MeV. Recently, E885 at the AGS [8] indicates a potential depth $V_0^\Xi = -14$ MeV or less. So the depth V_0^Ξ of Ξ in nuclear matter is not well fixed.

3 The effect of the Λ impurity

We start from the calculation of the single-particle energies for Λ in Λ-hypernuclei within the framework of the RMF model with force parameters taken from ref. [10], and present the results in fig. 1. It can be seen that the results are in good agreement with the experimental data [16–18]. Very small spin-orbit splittings for Λ-hypernuclei are also observed. This shows that the RMF theory with the parameter set used for the Λ hyperonic sector is reliable for studying the effect of the Λ impurity, and has a predicting power.

In order to observe the universality of the glue-like role of the Λ-hyperon impurity, a unified RMF calculation is needed and careful tests should be done. Hence, in our calculations, typical hypernuclei between $^{7}_{\Lambda}$Li and $^{209}_{\Lambda}$Pb are selected. Our results are shown in table 1, in which some

Table 1. Binding energy per baryon, $-E/A$ (in MeV), r.m.s. charge radius $r_{\rm ch}$ (those of the nucleons, in fm), r.m.s. radii of the hyperon (Λ, Ξ^-, Ξ^0), neutron and proton, $r_{\rm y}$, $r_{\rm n}$ and $r_{\rm p}$ (in fm), respectively, including the contribution of the ρ-mesons. The configuration of the hyperon is $1s_{1/2}$ for all hypernclei. Z in ${}^{A}Z$ stands for the number of protons. The results of the Ξ-hypernuclei are given in the form C^{+A}_{+B}, where C, $C+A$ and $C+B$ are the results obtained with $V_0^{\Xi} = -18, -10$ and -28 MeV, respectively.

${}^{A}Z$	$-E/A$	$r_{\rm ch}$	$r_{\rm y}$	$r_{\rm n}$	$r_{\rm p}$	${}^{A}Z$	$-E/A$	$r_{\rm ch}$	$r_{\rm y}$	$r_{\rm n}$	$r_{\rm p}$
^{6}Li	5.67	2.52		2.32	2.37	^{16}O	8.04	2.70		2.55	2.58
${}^{7}_{\Lambda}$Li	5.47	2.43	2.58	2.25	2.29	${}^{17}_{\Lambda}$O	8.27	2.70	2.43	2.55	2.58
${}^{7}_{\Xi^-}$Li	$5.18^{-0.27}_{+0.58}$	$2.39^{+0.07}_{-0.08}$	$3.20^{+1.55}_{-0.90}$	$2.35^{+0.00}_{-0.04}$	$2.25^{+0.07}_{-0.10}$	${}^{17}_{\Xi^-}$O	$8.14^{-0.29}_{+0.45}$	$2.67^{+0.02}_{-0.02}$	$2.59^{+0.74}_{-0.43}$	$2.58^{-0.01}_{-0.01}$	$2.55^{+0.01}_{-0.03}$
${}^{7}_{\Xi^0}$Li	$4.99^{-0.22}_{+0.56}$	$2.55^{-0.01}_{-0.04}$	$3.49^{+2.37}_{-1.13}$	$2.23^{+0.06}_{-0.09}$	$2.41^{-0.01}_{-0.04}$	${}^{17}_{\Xi^0}$O	$7.92^{-0.26}_{+0.44}$	$2.73^{-0.01}_{+0.00}$	$2.71^{+1.14}_{-0.51}$	$2.53^{+0.01}_{-0.03}$	$2.60^{+0.00}_{-0.00}$
^{8}Be	5.42	2.48		2.30	2.34	^{40}Ca	8.52	3.46		3.31	3.36
${}^{9}_{\Lambda}$Be	5.58	2.44	2.40	2.27	2.30	${}^{41}_{\Lambda}$Ca	8.75	3.46	2.70	3.31	3.36
${}^{9}_{\Xi^-}$Be	$5.30^{-0.32}_{+0.62}$	$2.41^{+0.04}_{-0.07}$	$2.80^{+1.22}_{-0.68}$	$2.33^{+0.00}_{-0.03}$	$2.26^{+0.04}_{-0.06}$	${}^{41}_{\Xi^-}$Ca	$8.75^{-0.16}_{+0.23}$	$3.44^{+0.00}_{-0.02}$	$2.75^{+0.49}_{-0.30}$	$3.33^{+0.00}_{-0.01}$	$3.34^{+0.01}_{-0.02}$
${}^{9}_{\Xi^0}$Be	$5.09^{-0.27}_{+0.60}$	$2.50^{+0.00}_{-0.02}$	$2.99^{+1.91}_{-0.83}$	$2.25^{+0.04}_{-0.07}$	$2.36^{+0.00}_{-0.02}$	${}^{41}_{\Xi^0}$Ca	$8.56^{-0.15}_{+0.23}$	$3.47^{+0.00}_{-0.00}$	$2.87^{+0.72}_{-0.37}$	$3.30^{+0.00}_{-0.02}$	$3.37^{+0.00}_{-0.00}$
^{12}C	7.47	2.46		2.30	2.32	^{208}Pb	7.90	5.51		5.71	5.45
${}^{13}_{\Lambda}$C	7.79	2.44	2.19	2.28	2.30	${}^{209}_{\Lambda}$Pb	7.98	5.51	4.05	5.71	5.44
${}^{13}_{\Xi^-}$C	$7.55^{-0.37}_{+0.65}$	$2.42^{+0.02}_{-0.04}$	$2.43^{+0.93}_{-0.51}$	$2.32^{+0.00}_{-0.02}$	$2.27^{+0.03}_{-0.04}$	${}^{209}_{\Xi^-}$Pb	$8.01^{-0.03}_{+0.05}$	$5.50^{+0.00}_{-0.01}$	$3.68^{+0.19}_{-0.13}$	$5.72^{+0.00}_{-0.01}$	$5.44^{+0.00}_{-0.01}$
${}^{13}_{\Xi^0}$C	$7.31^{-0.33}_{+0.63}$	$2.48^{+0.00}_{-0.01}$	$2.56^{+1.46}_{-0.60}$	$2.26^{+0.03}_{-0.04}$	$2.34^{+0.00}_{-0.01}$	${}^{209}_{\Xi^0}$Pb	$7.96^{-0.04}_{+0.05}$	$5.51^{+0.00}_{-0.00}$	$4.05^{+0.29}_{-0.20}$	$5.70^{+0.01}_{-0.00}$	$5.45^{+0.00}_{-0.00}$

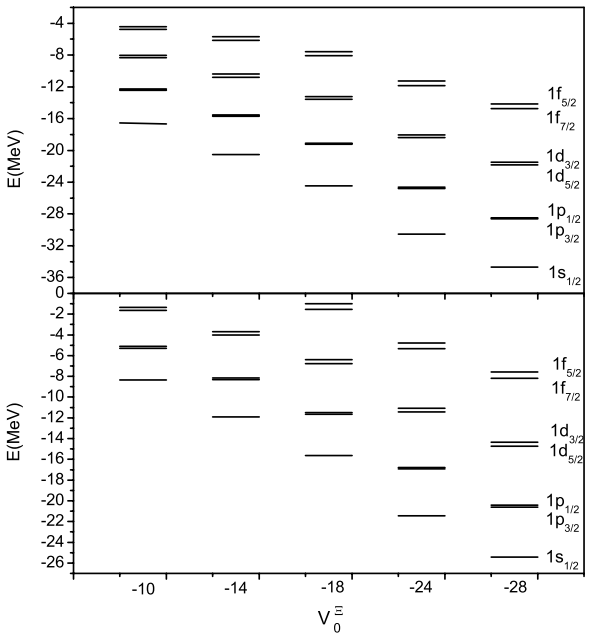

Fig. 2. Dependence of the position of the Ξ^- (upper part) and the Ξ^0 (lower part) single-particle levels in Zr for $V_0^{\Xi} = -10, -14, -18, -24, -28$ MeV (only the $1s, 1p, 1d, 1f$ states are given).

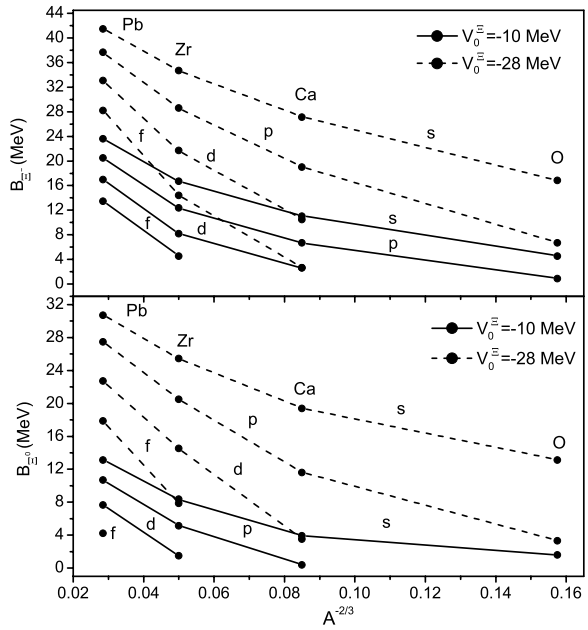

Fig. 3. Comparison of the Ξ^- (upper part) and the Ξ^0 (lower part) binding energies in O, Ca, Zr, Pb for $V_0^{\Xi} = -10$ and -28 MeV.

results for medium and heavy hypernuclei have been taken from our previous work [11]. In the table, $-E/A$ (in MeV) is the binding energy per baryon, $r_{\rm ch}$ is the r.m.s. charge radius, and $r_{\rm y}$, $r_{\rm n}$ and $r_{\rm p}$ are the calculated r.m.s. radii (in fm) of the hyperon (Λ or Ξ), neutron and proton, respectively. Here, the hyperon is in its $1s_{1/2}$ configuration. The definition of these quantities can be found in ref. [19]. For comparison, the results for normal nuclei are also given. From table 1, it can be seen that for a lighter Λ-hypernucleus, the size of the core nucleus in a hypernucleus is smaller than the core nucleus in free space (*i.e.*, normal nucleus). But the change in the core nucleus due to the presence of the Λ impurity is small though. For instance, the r.m.s. radius $r_{\rm n}$ ($r_{\rm p}$) of the neutrons (protons) decreases from 2.32 fm (2.37 fm) in ^{6}Li to 2.25 fm (2.29 fm)

Table 2. Binding energy per baryon, $-E/A$ (in MeV), r.m.s. charge radius $r_{\rm ch}$ (those of the nucleons, in fm), r.m.s. radii of the hyperon, neutron and proton, $r_{\rm y}$, $r_{\rm n}$ and $r_{\rm p}$ (in fm), respectively, including the contribution of the ρ-mesons. Z in ${}^{A}Z$ stands for the number of protons in hypernuclei. The configuration of the hyperon is $1s_{1/2}$ for all hypernuclei. The results of the Ξ-hypernuclei are given for $V_0^{\Xi} = -10, -18, -28$ MeV.

${}^{A}Z$	V_0^{Ξ}	$-E/A$	$r_{\rm ch}$	$r_{\rm y}$	$r_{\rm n}$	$r_{\rm p}$	${}^{A}Z$	V_0^{Ξ}	$-E/A$	$r_{\rm ch}$	$r_{\rm y}$	$r_{\rm n}$	$r_{\rm p}$
^{6}Li		5.67	2.52		2.32	2.37	^{16}O		8.04	2.70		2.55	2.58
${}^{7}_{\Xi^-}$Li	−10	4.91	2.46	4.75	2.35	2.32	${}^{17}_{\Xi^-}$O	−10	7.85	2.69	3.33	2.57	2.56
	−18	5.18	2.39	3.20	2.35	2.25		−18	8.14	2.67	2.59	2.58	2.55
	−28	5.76	2.31	2.30	2.31	2.15		−28	8.59	2.65	2.16	2.57	2.52
${}^{7}_{\Xi^0}$Li	−10	4.77	2.54	5.86	2.29	2.40	${}^{17}_{\Xi^0}$O	−10	7.66	2.72	3.85	2.54	2.60
	−18	4.99	2.55	3.49	2.23	2.41		−18	7.92	2.73	2.71	2.53	2.60
	−28	5.55	2.51	2.36	2.14	2.37		−28	8.36	2.73	2.20	2.50	2.60
^{8}Be		5.42	2.48		2.30	2.34	^{40}Ca		8.52	3.46		3.31	3.36
${}^{9}_{\Xi^-}$Be	−10	4.98	2.45	4.02	2.33	2.30	${}^{41}_{\Xi^-}$Ca	−10	8.59	3.44	3.24	3.33	3.35
	−18	5.30	2.41	2.80	2.33	2.26		−18	8.75	3.44	2.75	3.33	3.34
	−28	5.92	2.34	2.12	2.30	2.20		−28	8.98	3.42	2.45	3.32	3.32
${}^{9}_{\Xi^0}$Be	−10	4.82	2.50	4.90	2.29	2.36	${}^{41}_{\Xi^0}$Ca	−10	8.41	3.47	3.59	3.30	3.37
	−18	5.09	2.50	2.99	2.25	2.36		−18	8.56	3.47	2.87	3.30	3.37
	−28	5.69	2.48	2.16	2.18	2.34		−28	8.79	3.47	2.50	3.28	3.37
^{12}C		7.47	2.46		2.30	2.32	^{208}Pb		7.90	5.51		5.71	5.45
${}^{13}_{\Xi^-}$C	−10	7.18	2.44	3.36	2.32	2.30	${}^{209}_{\Xi^-}$Pb	−10	7.98	5.50	3.87	5.72	5.44
	−18	7.55	2.42	2.43	2.32	2.27		−18	8.01	5.50	3.68	5.72	5.44
	−28	8.20	2.38	1.92	2.30	2.23		−28	8.06	5.49	3.55	5.71	5.43
${}^{13}_{\Xi^0}$C	−10	6.98	2.48	4.02	2.29	2.34	${}^{209}_{\Xi^0}$Pb	−10	7.92	5.51	4.34	5.71	5.45
	−18	7.31	2.48	2.56	2.26	2.34		−18	7.96	5.51	4.05	5.70	5.45
	−28	7.94	2.47	1.96	2.22	2.33		−28	8.01	5.51	3.85	5.70	5.45

Table 3. Binding energy per baryon, $-E/A$ (in MeV), r.m.s. charge radius $r_{\rm ch}$ (those of the nucleons, in fm), r.m.s. radii of the hyperon, neutron and proton, $r_{\rm y}$, $r_{\rm n}$ and $r_{\rm p}$ (in fm), respectively, without the contribution of the ρ-mesons. Z in ${}^{A}Z$ stands for the number of protons. The configuration of the hyperon is $1s_{1/2}$ for all hypernuclei. The results of the Ξ-hypernuclei are given in the form C^{+A}_{+B}, where C, $C+A$ and $C+B$ are the results obtained with $V_0^{\Xi} = -18, -10$ and -28 MeV, respectively.

${}^{A}Z$	$-E/A$	$r_{\rm ch}$	$r_{\rm y}$	$r_{\rm n}$	$r_{\rm p}$	${}^{A}Z$	$-E/A$	$r_{\rm ch}$	$r_{\rm y}$	$r_{\rm n}$	$r_{\rm p}$
^{6}Li	5.67	2.52		2.32	2.37	^{16}O	8.04	2.70		2.55	2.58
${}^{7}_{\Xi^-}$Li	$5.27^{-0.32}_{+0.68}$	$2.44^{+0.05}_{-0.07}$	$2.82^{+1.35}_{-0.75}$	$2.27^{+0.04}_{-0.07}$	$2.30^{+0.05}_{-0.08}$	${}^{17}_{\Xi^-}$O	$8.19^{-0.31}_{+0.47}$	$2.70^{+0.01}_{-0.02}$	$2.46^{+0.67}_{-0.39}$	$2.55^{+0.01}_{-0.02}$	$2.57^{+0.01}_{-0.01}$
${}^{7}_{\Xi^0}$Li	$5.06^{-0.27}_{+0.64}$	$2.46^{+0.04}_{-0.07}$	$3.04^{+2.12}_{-0.91}$	$2.28^{+0.03}_{-0.07}$	$2.32^{+0.05}_{-0.08}$	${}^{17}_{\Xi^0}$O	$7.94^{-0.27}_{+0.46}$	$2.70^{+0.01}_{-0.01}$	$2.60^{+1.03}_{-0.48}$	$2.55^{+0.01}_{-0.01}$	$2.58^{+0.00}_{-0.02}$
^{8}Be	5.42	2.48		2.30	2.34	^{40}Ca	8.52	3.46		3.31	3.36
${}^{9}_{\Xi^-}$Be	$5.39^{-0.37}_{+0.69}$	$2.44^{+0.03}_{-0.05}$	$2.54^{+1.05}_{-0.59}$	$2.28^{+0.02}_{-0.05}$	$2.30^{+0.03}_{-0.05}$	${}^{41}_{\Xi^-}$Ca	$8.77^{-0.17}_{+0.24}$	$3.45^{+0.01}_{-0.01}$	$2.65^{+0.45}_{-0.29}$	$3.31^{+0.00}_{-0.01}$	$3.35^{+0.01}_{-0.01}$
${}^{9}_{\Xi^0}$Be	$5.16^{-0.33}_{+0.66}$	$2.45^{+0.03}_{-0.05}$	$2.71^{+1.62}_{-0.71}$	$2.28^{+0.03}_{-0.05}$	$2.31^{+0.03}_{-0.05}$	${}^{41}_{\Xi^0}$Ca	$8.56^{-0.15}_{+0.23}$	$3.46^{+0.00}_{-0.01}$	$2.84^{+0.74}_{-0.37}$	$3.31^{+0.00}_{-0.01}$	$3.36^{+0.00}_{-0.01}$
^{12}C	7.47	2.46		2.30	2.32	^{208}Pb	7.90	5.51		5.71	5.45
${}^{13}_{\Xi^-}$C	$7.63^{-0.41}_{+0.71}$	$2.44^{+0.02}_{-0.03}$	$2.26^{+0.82}_{-0.47}$	$2.28^{+0.01}_{-0.03}$	$2.30^{+0.02}_{-0.03}$	${}^{209}_{\Xi^-}$Pb	$8.00^{-0.07}_{+0.09}$	$5.50^{+0.01}_{-0.00}$	$4.64^{+2.15}_{-1.22}$	$5.71^{+0.00}_{-0.01}$	$5.45^{+0.00}_{-0.01}$
${}^{13}_{\Xi^0}$C	$7.37^{-0.37}_{+0.68}$	$2.45^{+0.01}_{-0.03}$	$2.38^{+1.24}_{-0.55}$	$2.29^{+0.01}_{-0.04}$	$2.31^{+0.01}_{-0.03}$	${}^{209}_{\Xi^0}$Pb	$7.93^{-0.03}_{+0.05}$	$5.51^{+0.00}_{-0.01}$	$4.17^{+0.47}_{-0.26}$	$5.71^{+0.00}_{-0.00}$	$5.44^{+0.01}_{-0.00}$

in ${}^{7}_{\Lambda}$Li. We also see from the table that the change of $r_{\rm n}$ and $r_{\rm p}$ gradually decreases with increasing mass number. The above RMF results reveal the universality of the shrinkage effect for the Λ-hypernuclei, but not for the Ξ-hypernuclei. It is particularly interesting to observe a quite different effect caused by the Ξ-hyperon impurity.

4 The effect of the Ξ impurity

In order to see whether or not there is the shrinkage effect of the Ξ-hypernuclei, we have carried out the standard RMF calculations for some Ξ^-- and Ξ^0-hypernuclei. Due to the insufficient experimental information on

Ξ-hypernuclei, the Ξ potential well depth is relatively uncertain, the values appearing in the literature range from about -30 to -10 MeV. Recent experiments with light nuclei suggest that the value lies on the less bound size of this range [8,15]. However, it may be more deeply bound for heavy nuclei [20]. As a result, a number of values of the Ξ potential well depth V_0^{Ξ} for each hypernuclei are used to test the sensitivity of the position of Ξ single-particle energy levels to the potential depth. In fig. 2, we only present results of calculations for the nucleus Zr with a comparison of the Ξ^- (upper part) and the Ξ^0 (lower part) single-particle levels. It can be seen that the change of the potential well depth causes a large change in the single-particle energies. As V_0^{Ξ} becomes deeper, the single-particle energies of the hyperon increase significantly, and the spin-orbit splitting gets a little larger. We also see that the attractive Coulomb interaction for Ξ^- leads to a considerably stronger binding of Ξ^- in nuclei when compared with Ξ^0-hypernuclei. In fig. 3, we give the Ξ^- (upper part) and Ξ^0 (lower part) binding energies in the nuclei O, Ca, Zr, Pb for $V_0^{\Xi} = -10$ and -28 MeV (only the $1s, 1p, 1d, 1f$ states are given). The solid (dashed) curves are the results for $V_0^{\Xi} = -10$ (-28) MeV.

Next, let us go further into the question of how the static properties of the Ξ-hypernuclei are affected by the potential depth V_0^{Ξ}. Both Ξ^- and Ξ^0 are in the $1s$ state in hypernuclei. Our RMF results are shown in table 2 with $V_0^{\Xi} = -10, -18$ and -28 MeV, respectively. As seen from table 2, with increasing the depth $|V_0^{\Xi}|$ from 10 MeV to 28 MeV, the binding energies per baryon ($-E/A$) become larger. We can see that such an uncertainty of the Ξ potential well depth is clearly reflected in an important variation of the Ξ binding energies, as is shown in figs. 2 and 3 and also of the binding energies per baryon ($-E/A$), presented in table 2. Because of that, no firm conclusions can be drawn from the quoted values of $-E/A$. We can also notice that the charge radius and the r.m.s. radii of the Ξ-hyperon, neutrons and protons become smaller with increasing potential well depth. Note that the reduction of the r.m.s. radius for the neutrons ($r_{\rm n}$) and protons ($r_{\rm p}$) is different. In the case of Ξ^--hypernuclei, the reduction of $r_{\rm p}$ is faster than that of $r_{\rm n}$. While in the case of Ξ^0-hypernuclei, the reduction of $r_{\rm p}$ is slower than that of $r_{\rm n}$. Thus, the RMF model predicts that the proton and neutron distributions have different response to the potential depth V_0^{Ξ} for the Ξ^-- and Ξ^0-hypernuclei.

Now, we study whether the Ξ-hyperon impurity has a glue-like role as Λ does. The results are shown in table 1 in the form C^{+A}_{+B}, where the central values (C) are the results obtained with the -18 MeV Ξ potential well depth, while the extremes of the uncertainty interval $C+A$ and $C+B$ are obtained with $V_0^{\Xi} = -10$ MeV and -28 MeV, respectively. A similar presentation is used in table 3 (where the ρ exchange is not considered, *i.e.*, $g_{\rho\Xi} = 0$). From table 1, we find that, by adding a Ξ^--hyperon to the nuclei, the r.m.s. radius of the neutrons becomes a little larger, while the r.m.s. radius of the protons becomes much smaller, in comparison with that in normal nuclei. In contrast to the situation of the Ξ^--hypernuclei, by adding a Ξ^0-hyperon, the r.m.s. radius of the protons becomes larger and that of the neutrons becomes smaller. This is different from the situation of adding a Λ-hyperon. We know that Λ has a glue-like role, both the r.m.s. radii of the protons and neutrons become smaller when adding a Λ. Note that Λ, Ξ^- and Ξ^0 are particles different from proton and neutron, they are all not constrained by the Pauli exclusion principle; it is obvious that the common explanation for the shrinkage does not suit the case of Ξ^- and Ξ^0. Otherwise, both Λ- and Ξ^0-hyperons are neutral, hence the origin of the above difference cannot be attributed to the Coulomb potential. There must be some other source that we do not recognize.

To reach a better understanding of the different behavior of the Λ, Ξ^- and Ξ^0 impurities in the nucleus, we make an inspection of their isospin. Λ, Ξ^- and Ξ^0 have a different third component of isospin, which may be responsible for their different behavior. The different third component of isospin works through the coupling of baryon with the ρ-mesons in the RMF model. We may imagine that if the ρ-mesons couplings for Ξ^- and Ξ^0 are omitted from the RMF calculation ($g_{\rho\Xi} = 0$), the above-mentioned different behavior of Ξ^- and Ξ^0 shall disappear. After eliminating the contribution of the ρ-mesons, the RMF results are shown in table 3, from which we find that the r.m.s. radii of both the protons and neutrons reduce when adding a Ξ^-- or a Ξ^0-hyperon to the normal nuclei, the same as the situation of adding a Λ-hyperon. We obtain the same nuclear shrinkage by Ξ^- and Ξ^0 when ignoring the contribution of the ρ-mesons. From the interactive term of nucleons with the ρ-mesons, we can find that, when adding a Ξ^-, the attractive force increases for the protons and the repulsive force increases for the neutrons, the situation is contrary to the above when adding a Ξ^0. And this explains the above RMF results reasonably. So, we can conclude that the ρ-mesons play an important role, and the different behavior of the Λ, Ξ^- and Ξ^0 impurities is due to their different isospin. Although the changes are small, the different response of $r_{\rm p}$ and $r_{\rm n}$ to Ξ^- and Ξ^0 may be interesting to know what kind of properties the two-body ΞN interaction has. Probably the isospin $T = 0$ interaction is attractively large, while the $T = 1$ interaction is repulsive and small. However, the r.m.s. radius is reduced only for one kind of nucleons, but the r.m.s radius of the other kind of nucleons becomes larger, that is it seems that the nuclei may even swell somewhat when adding a Ξ^- or a Ξ^0. That is very different from the nuclear shrinkage by Λ.

5 Summary and conclusion

Within the framework of the RMF theory, the Λ single-particle energies were calculated and the results are in good agreement with the experiments for all of the hypernuclei considered. Very small spin-orbit splittings for Λ-hypernuclei are observed, which is in agreement with earlier phenomenological analysis. From the investigation of the effects of Λ on the core nucleus, we obtain the shrinkage effect induced by the Λ-hyperon impurity, otherwise, we find that other light and medium Λ-hypernuclei also

have this shrinkage effect, *i.e.*, the glue-like role of the Λ impurity is universal.

For Ξ-hypernuclei, first, we study the effect of the potential well depth V_0^{Ξ} on the static properties of the Ξ-hypernuclei. We can see that the uncertainty of the Ξ potential well depth gets clearly reflected in an important variation of the Ξ binding energies; because of that, no firm conclusions can be drawn from the quoted Ξ binding energies and values of $-E/A$. In the Ξ^--hypernuclei, the reduction of the r.m.s. radius of the protons is larger than the reduction of that of the neutrons, while in the Ξ^0-hypernuclei, the reduction of the r.m.s. radius of the neutrons is larger than that of the protons with a deeper potential well depth. The strength of the effect of V_0^{Ξ} on different nucleons is different in Ξ-hypernuclei. The effect of V_0^{Ξ} on the hypernuclei decreases with increasing atomic number.

After that, we study the effect of adding the Ξ-hyperon on the nuclear core; we find that by adding a Ξ^--hyperon to the nucleus, the r.m.s. radius of the neutrons becomes a little larger, while the r.m.s. radius of the protons becomes smaller, in comparison with that in the normal nucleus, and the decrease of the r.m.s. radius of the protons is larger as V_0^{Ξ} becomes deeper. Whereas when adding a Ξ^0-hyperon, the r.m.s. radius of the protons becomes a little larger and that of the neutrons becomes smaller. The r.m.s. radius is reduced only for one kind of nucleon, the r.m.s radius of the other kind of nucleon becomes larger, that is it seems that the nuclei may even swell somewhat when adding a Ξ^- or a Ξ^0. And this is very different from the nuclear shrinkage by Λ. Moreover we find that the ρ-mesons play an important role, the different effect on the nuclear core by Λ, Ξ^-, Ξ^0 is due to their different isospin. Although the changes are small, the different response of $r_{\rm p}$ and $r_{\rm n}$ to Ξ^- and Ξ^0 may be interesting to know what kind of properties the two-body ΞN interaction has. Probably the isospin $T = 0$ interaction is attractively large, while the $T = 1$ interaction is repulsive and small.

The present work only focuses on the pure Λ- and Ξ-hypernuclei, the coupling between ΞN and $\Lambda\Lambda$ channels in Ξ-hypernuclei is not taken into consideration. The physics of $\Lambda\Lambda$-hypernuclei ($\Lambda\Lambda$ and ΞN mix up in a formalism of coupled channel) and of the $\Lambda\Xi$-hypernuclei has attracted a lot of attention [21] and is subject of current investigation; because of that, more reliable information on the ΞN interaction and the Ξ-nucleus is desired.

This work was supported in part by China postdoctoral science foundation (2002032169), National Natural Science Foundation of China (10275037) and China Doctoral Programme Foundation of the Institution of Higher Education (20010055012). We would like also to thank Prof. Chonghai Cai, Prof. Lei Lee and Baoxi Sun for useful discussions.

References

1. T. Motoba, H. Bandō, K. Ikeda, Prog. Theor. Phys. **80**, 189 (1983).
2. E. Hiyama *et al.*, Phys. Rev. C **53**, 2075 (1996).
3. E. Hiyama, M. Kamimura, K. Miyazaki, T. Motoba, Phys. Rev. C **59**, 2351 (1999).
4. K. Tanida, H. Tamura, D. Abe *et al.*, Nucl. Phys. A **684**, 560 (2001).
5. K. Tanida, H. Tamura, D. Abe *et al.*, Phys. Rev. Lett. **86**, 1982 (2001).
6. S. Bart *et al.*, Phys. Rev. Lett. **83**, 5238 (1999).
7. H. Noumi *et al.*, Phys. Rev. Lett. **89**, 072301 (2002).
8. P. Khaustov *et al.*, Phys. Rev. C **61**, 054603 (2000).
9. M.M. Sharma, M.A. Nagarajan, P. Ring, Phys. Rev. Lett. B **312**, 377 (1993).
10. Z.Y. Ma, J. Speth, S. Krewald *et al.*, Nucl. Phys. A **608**, 305 (1996).
11. Yu Hong Tan, Yan An Luo, Ping Zhi Ning, Zhong Yu Ma, Chin. Phys. Lett. **18**, 1030 (2001).
12. N.K. Glendenning, S.A. Moszkowski, Phys. Rev. Lett. **67**, 2414 (1991).
13. J. Schaffner, C. Greiner, H. Stöcker, Phys. Rev. C **46**, 322 (1992).
14. C.B. Dover, A. Gal, Ann. Phys. (N.Y.) **146**, 309 (1983).
15. T. Fukuda *et al.*, Phys. Rev. C **58**, 1306 (1998).
16. S. Ajimura *et al.*, Nucl. Phys. A **585**, 173 (1995).
17. Q.N. Usmani, A.R. Bodmer, Phys. Rev. C **60**, 055215 (1999).
18. P.H. Pile, S. Bart, R.E. Chrien *et al.*, Phys. Rev. Lett. **66**, 2585 (1991).
19. Y.K. Gambhir, P. Ring, A. Thimet, Ann. Phys. (N.Y.) **198**, 132 (1990).
20. Y. Yamamoto *et al.*, Prog. Theor. Phys. Suppl. **117**, 361 (1994).
21. C. Albertus, J.E. Amaro, J. Nieves, Phys. Rev. Lett. **89**, 032501 (2002); I.N. Filikhin, A. Gal, Phys. Rev. C **65**, 041001 (2002); S.B. Carr, I.R. Afnan, B.F. Gibson, Nucl. Phys. A **625**, 143 (1997); T. Yamada, C. Nakamoto, Phys. Rev. C **62**, 034319 (2000).